ELSEVIER

Materials Science and Engineering A 483–484 (2008) 637–640

MATERIALS SCIENCE & ENGINEERING A

www.elsevier.com/locate/msea

Grain-size stabilization by impurities and effect on stress-coupled grain growth in nanocrystalline Al thin films

D.S. Gianola [a], B.G. Mendis [a], X.M. Cheng [b], K.J. Hemker [a,*]

[a] *Department of Mechanical Engineering, Johns Hopkins University, Baltimore, MD 21218, United States*
[b] *Department of Physics & Astronomy, Johns Hopkins University, Baltimore, MD 21218, United States*

Received 6 June 2006; received in revised form 22 September 2006; accepted 3 December 2006

Abstract

Room-temperature tensile experiments on sub-micrometer freestanding thin films deposited at varied base pressures reveal two distinct classes of mechanical response. Samples that contain sufficient impurity concentrations to stabilize the microstructure against an applied stress show strong but brittle response. However, films that were deposited at lower vacuum base pressures that still allow for thermally stable nanostructures show remarkably different deformation response; namely, moderate strength and over 15% plastic strain to failure. Post-mortem transmission electron microscopy of deformed samples with different levels of impurity pinning atmospheres reveals stress-driven discontinuous grain growth that facilitates a fundamental change in the deformation behavior of these thin films. The results indicate a critical impurity concentration to sufficiently pin or immobilize grain boundaries against the coupling of applied stresses.

Keywords: Nanocrystalline materials; Impurity drag; Grain boundary migration; Thin films; Mechanical properties

1. Introduction

In the wake of growing interest in nanocrystalline (nc) materials spawned by measurements of superior mechanical properties, the thermal stability of these nanostructures has been questioned [1–4]. The large volume fraction of grain boundaries has been shown to promote microstructural instabilities (grain growth) at temperatures much lower than bulk recrystallization temperatures [1] or even spontaneously (i.e. room temperature) [5]. Nonetheless, several researchers have shown that impurities can play a large role in stabilizing nanocrystalline microstructures by reducing the mobility of grain boundaries under thermal loads [6–8].

Evidence is emerging that underscores the influence of the applied stress on microstructural evolution in nc-metals, even when the material exhibits thermal stability or is deformed in the absence of thermal activation (cryogenic temperatures) [9]. Recent examples of this phenomenon describe observations of rapid grain coarsening [10,11]. Theoretical formulations have recently been developed that directly correlate applied shear stresses to normal grain boundary migration [12,13]. This ability of shear stresses to directly couple to low and high angle grain boundaries [14,15] and the ensuing grain growth has been shown to have a dramatic effect on the mechanical behavior of nc-Al [16,17]. Although the details surrounding the underlying mechanistic processes have yet to be elucidated, the unpinning of grain boundaries from impurity atmospheres appears to govern the distinct change in behavior that follows stress-coupled microstructural evolution [16].

The effect of chamber base pressure during physical vapor deposition processes on the grain size of pure metallic thin films is well documented [18]; the higher the base pressure, the higher the impurity concentration, resulting in smaller grain sizes. However, the processes surrounding the coupling of stresses to the motion of grain boundaries and the role of impurities in these activities are still not known. Here we systematically vary the base pressure during sputtering of submicron Al thin films and investigate the tensile behavior and corresponding microstructures before and after deformation in an effort to elucidate the function of impurities in controlling against the driving force of stress-coupled grain boundary motion.

2. Material synthesis and experimental methods

Submicron freestanding thin films were synthesized [16] using pulsed dc magnetron sputtering of a 99.999% pure Al

* Corresponding author. Tel.: +1 410 516 4489; fax: +1 410 516 7254.
E-mail address: hemker@jhu.edu (K.J. Hemker).

0921-5093/$ – see front matter © 2007 Elsevier B.V. All rights reserved.
doi:10.1016/j.msea.2006.12.155

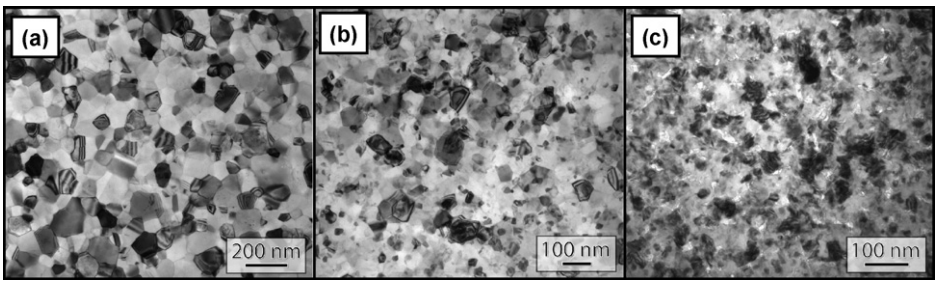

Fig. 1. TEM images of as-deposited Al films deposited at base pressures of approximately: (a) 10^{-7}, (b) 10^{-6}, and (c) 10^{-5} mmHg.

target at varied base chamber pressures of between 10^{-7} and 10^{-5} mmHg in order to introduce varying amounts of impurities. A tensile testing structure, designed and constructed using Si-based microfabrication techniques [16], provided a rigid frame for handling and mounting fragile freestanding thin films. A custom built microsample tensile testing apparatus was utilized for mechanical testing (details on this setup can be found in [19]). Strain was measured locally in the gage section of the sample using a custom digital image tracking system, using fine silica powder as markers for tracking [20].

Al films with nominal thicknesses of 180 nm were strained in tension at a constant strain rate of $4 \times 10^{-5}\ s^{-1}$. Post-mortem transmission electron microscopy (TEM) was employed to measure grain size distributions of a minimum of 200 grain measurements before and after deformation. Representative TEM images of the grain morphology of films deposited at all three base pressures are shown in Fig. 1. Mean grain sizes for the as-deposited films are listed in Table 1 and were calculated using equivalent circle diameters from direct grain area measurements. It should be noted that grain size measurements of the films deposited at approximately 10^{-5} mmHg was difficult due to the small sizes and number of overlapping grains through the thickness of the films, increasing the uncertainty of these measurements.

Elemental composition, film thickness, and roughness are given in Table 1. While the absolute values of the O content as measured by scanning electron microscope; energy-dispersive spectrometry (SEM-EDS) appear to be high based on a calculation of a native oxide layer on the surface of the films, a trend based on base pressure (although no dependence of film thickness or roughness) is still observed. This discrepancy of the measurement is attributed to the difficulties associated with making well-calibrated measurements of light elements. Auger depth profiling was carried out by argon ion sputtering through the depth of a film deposited at a base pressure of 10^{-7} mmHg, where oxygen was found to be concentrated only at the surface as a native oxide layer. No buried oxide layers, which may have formed during pulsed deposition, were observed within the detection limit of the experimental technique.

The existence of second phases and amorphous films at grain boundaries of pure nanocrystalline materials have been hypothesized and predicted to have a significant impact on the stability and mechanical response [21]. However, detailed high-resolution TEM images of grain boundaries (Fig. 2) of Al films reveal atomically sharp interfaces in which crystallinity is maintained up to the boundary. Moreover, no second-phase particles or precipitates were detected. As such, the discussion of impurity pinning and grain boundary drag will be restricted to solute impurities.

3. Results and discussion

Representative mechanical responses for the Al films deposited at different base pressures are shown in Fig. 3 as obtained from tensile testing. A clear distinction in deformation behavior was measured between the films deposited at approximately 10^{-5} mmHg and those synthesized at both 10^{-6} and 10^{-7} mmHg. Namely, films deposited at the highest chamber pressure are strong (over 25 times stronger than microcrystalline Al) but brittle. This behavior agrees with reported literature of mechanical properties of nc-fcc metals, in which high strengths are typically obtained at the expense of ductility [22–24]. This class of behavior is usually attributed to the difficulty of operating intragranular dislocation sources and the suppression of dislocation interactions. A contrasting behavior is measured from the films deposited at base pressures of 10^{-6} and 10^{-7} mmHg, where large amounts of plastic strain (in excess of 15%) were obtained. These films show apparent work hardening in early stages of deformation followed by a sharp yield point that extends to a region of constant work hardening for films deposited at 10^{-7} mmHg and slowly diminishing stress until failure for those deposited at 10^{-6} mmHg. The difference in flow stress between these two films arises from the difference in initial grain size. The results shown in Fig. 3 imply that a criti-

Table 1
Properties of sputtered Al thin films

Base pressure (mmHg)	Al (at.%)	O (at.%)	Thickness (nm)	Film roughness, R_a (nm)	Initial mean grain size (nm)
2.2×10^{-7}	97.08 ± 0.15	2.92 ± 0.15	181 ± 11	<4	61 ± 28
3.0×10^{-6}	96.28 ± 0.16	3.72 ± 0.16	172 ± 5	<2	29 ± 20
1.1×10^{-5}	90.18 ± 0.15	9.82 ± 0.15	184 ± 6	<3	13 ± 8

Compositions determined using SEM-EDS.

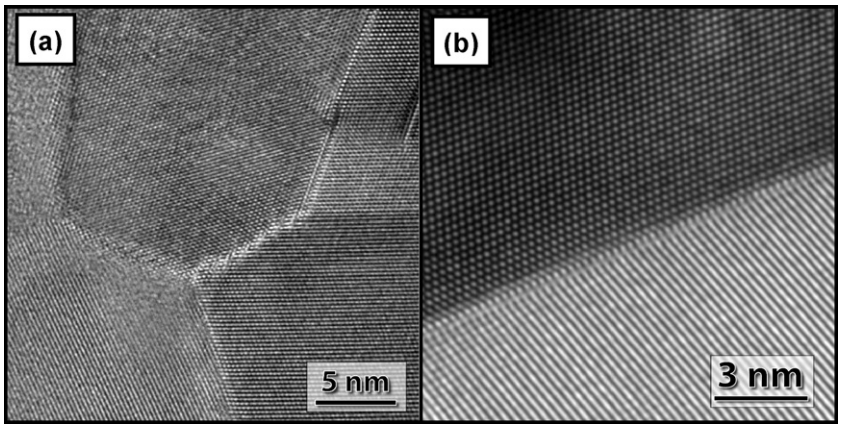

Fig. 2. High resolution transmission electron micrographs of Al films deposited at a base pressure of approximately 10^{-7} mmHg showing atomically sharp grain boundaries. There is no evidence of second-phase particles in the bulk or at the grain boundary.

cal transition from one type of behavior to the other is a function of the deposition base pressure and the corresponding impurity level.

Post-mortem grain size measurements of all films in the as-deposited condition and after deformation are shown in Fig. 4 in the form of a cumulative distribution function, where the vertical axis represents the area fraction of grains that are less than a given grain size. The difference in the as-deposited grain size distributions given numerically in Table 1 are visually represented in Fig. 4. Examination of these grain size distributions clearly shows microstructural evolution for the films deposited at 10^{-6} and 10^{-7}, while the distribution of the film that demonstrated strong and brittle response (10^{-5} mmHg) mimics that of its as-deposited condition. Hence, there is a correlation between extended ductility and whether or not grain growth has occurred. In addition, grain sizes measured outside of the deformed region of specimens that exhibited grain growth are similar to the initial state, suggesting that the evolution is directly tied to the applied stress or deformation in the sample. TEM images of the grain morphology in deformed samples show that the growth is discontinuous in nature; large grains seem to have grown at the expense of small ones. Moreover, the maximum grain size measured did not depend on the initial distribution, and scales with about 2–3 times the film thickness, which is a well-characterized thin film effect [16,18].

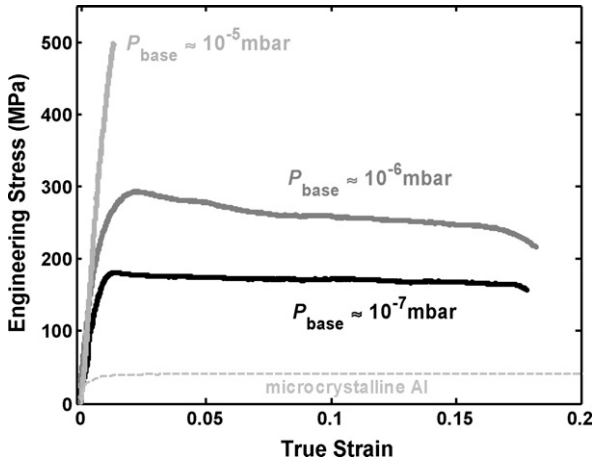

Fig. 3. Room temperature tensile stress–strain curves for the three batches of Al films, showing two distinct classes of mechanical behavior.

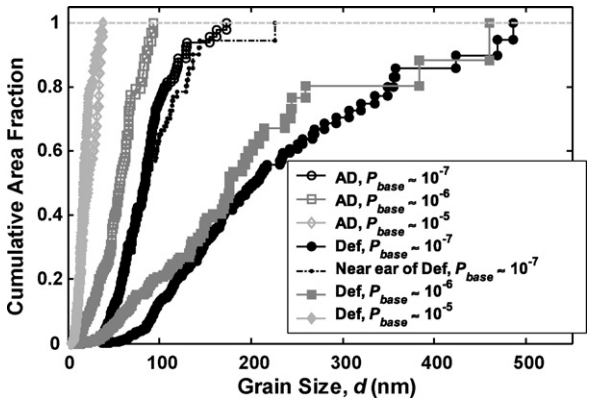

Fig. 4. Cumulative grain size distribution functions for as-deposited (AD, open symbols) and deformed (Def, filled symbols) Al films, where the ordinate represents the area fraction of grains that are less than a given grain size. Base pressures in mmHg.

4. Conclusion

The effect of impurity concentration, as controlled by adjusting the vacuum base pressure during deposition of nc-Al thin films, on the nanostructural stability against an applied stress at room temperature was measured. The tensile behavior of specimens that exhibit stress-coupled grain growth during deformation was shown to be dramatically different than that of samples showing no nanostructural evolution. Namely, extended ductility and intermediate strengths can be obtained if the stress can couple to the grain boundaries and liberate the interface from the local impurity pinning atmosphere, causing discontinuous grain growth. The results presented here demonstrate the potential for controlling this nanostructural instability with impurities and subsequently tailoring the material for desired mechanical response.

Acknowledgements

This work was supported by an NSF NIRT Program (Grant No. DMR-0210215). The authors thank Chris Eberl and Scott Hoffmann for their technical assistance.

References

[1] B.S. Günther, A. Kumpmann, H.-D. Kunze, Scripta Metall. Mater. 27 (1992) 833.
[2] R. Mitra, et al., in: Y.-W. Chung, D.C. Dunand, P.K. Liaw, G.B. Olson (Eds.), Advanced Materials for the 21st Century, TMS, Warrendale, PA, 1999, p. 553.
[3] J. Weissmüller, Nanostruct. Mater. 3 (1993) 261.
[4] T.R. Malow, C.C. Koch, Mater. Sci. Forum 225 (1996) 595.
[5] J.A. Haber, W.E. Buhro, J. Am. Chem. Soc. 120 (1998) 10847.
[6] L.A. Zepeda-Ruiz, et al., Appl. Phys. Lett. 87 (2005) 231904.
[7] J. Weissmüller, et al., Nanostruct. Mater. 1 (1992) 439.
[8] P.C. Millett, R.P. Selvam, A. Saxena, Acta Mater. 54 (2006) 297.
[9] K. Zhang, J.R. Weertman, J.A. Eastman, Appl. Phys. Lett. 87 (2005) 061921.
[10] M. Jin, A.M. Minor, E.A. Stach, J.W. Morris Jr., Acta Mater. 52 (2004) 5381.
[11] K. Zhang, J.R. Weertman, J.A. Eastman, Appl. Phys. Lett. 85 (2004) 5197.
[12] J.W. Cahn, J.E. Taylor, Acta Mater. 52 (2004) 4887.
[13] M.Yu. Gutkin, I.A. Ovid'ko, Appl. Phys. Lett. 87 (2005) 251916.
[14] M. Winning, G. Gottstein, L.S. Shvindlerman, Acta Mater. 49 (2001) 211.
[15] M. Winning, G. Gottstein, L.S. Shvindlerman, Acta Mater. 50 (2002) 353.
[16] D.S. Gianola, et al., Acta Mater. 54 (2006) 2263.
[17] D.S. Gianola, D.H. Warner, J.F. Molinari, K.J. Hemker, Scripta Mater. 50 (2006) 649.
[18] C.V. Thompson, Annu. Rev. Mater. Sci. 30 (2000) 159.
[19] D.S. Gianola, K.J. Hemker, M. Legros, W.N. Sharpe Jr., TMS Lett. 1 (2004) 149.
[20] W.N. Sharpe Jr., et al., Proceedings of ASME Annual Meeting, #IMECE2006-13290, 2006.
[21] M.A. Meyers, E. Ashworth, Phil. Mag. A 46 (1982) 737.
[22] H.D. Espinosa, B.C. Prorok, B. Peng, J. Mech. Phys. Solids 52 (2004) 667.
[23] M.A. Haque, M.T.A. Saif, Proc. Natl. Acad. Sci. U.S.A. 101 (2004) 6335.
[24] P.G. Sanders, J.A. Eastman, J.R. Weertman, Acta Mater. 45 (1997) 4019.